Hurricane Risk of Solar Generation in the United States

Luis Ceferino, A.M.ASCE[1]; and Ning Lin, A.M.ASCE[2]

Abstract: Projections indicate that solar energy will constitute 55% of total electricity capacity by 2050 in the US. Despite solar energy's growing importance, few studies have analyzed the risks of countrywide deployments of solar infrastructure due to extreme weather events such as hurricanes. This paper presents a probabilistic framework to evaluate the performance of solar infrastructure to generate energy during hurricanes, which often cause significant outages in the US. Our novel framework integrates recent data-driven models that capture two critical and compounding factors: transient cloud conditions that decrease irradiance and high winds that can cause permanent panel damage. We apply the framework to the 2,694 counties in the 38 central and eastern US states to elucidate the risk landscape of solar generation during hurricanes. Our results show that hurricane impacts are significant, compounding, and strikingly disproportional in the US. We show that in Florida and Louisiana, clouds rapidly reduce solar generation to 32% and 65%, respectively, of their normal levels with a return period of 100 years. Our results also show that damage to panels can induce more acute and permanent energy losses, especially in rarer storms, e.g., causing 80% more losses than hurricane clouds 2 days after landfall for 200-year events. **DOI: 10.1061/NHREFO.NHENG-1764.**

Author keywords: Solar panels; Energy resilience; Hurricane risk; Solar irradiance; Wind damage.

Introduction

Ensuring continuous electricity delivery is key to supporting communities in responding and recovering from extreme natural events. Nevertheless, the grid is far from resilient. Hurricane Maria in 2017, for example, caused one of the longest and largest power outages in the modern US, which left half of Puerto Rico without power for at least 4 months (Wang et al. 2018). Last year, Hurricane Ida damaged 30,000 utility poles, leaving 1.2 million customers without power across eight states (Boyle 2021), ranking as the costliest disaster in the world in 2021 (Swiss Re Institute 2022).

Governments are investing aggressively in upgrading the grid to enhance resilience. Through the Bipartisan Infrastructure Law, the US Department of Energy (DOE) will provide USD 2.3 billion over the next 5 years to strengthen US power systems against extreme weather (White House 2022). Furthermore, through the Bipartisan Infrastructure Law and the 2022 Energy Act, the US will invest even more ambitiously (USD 62 billion) in accelerating renewable adoption, including solar energy, to achieve net-zero electricity by 2035 and become a net-zero economy by 2050 (Department of Energy 2022). Motivated by the need to plan for these large-scale investments holistically, this paper studies the large-scale risk landscape of solar generation to hurricanes across the entire central and eastern US.

We focus on solar panels because the US Energy Information Administration (EIA) projects them to constitute 55% of total electricity capacity by 2050 (US Energy Information Administration 2022) and also because they have a high potential to increase resilience when deployed as a distributed energy resource. In fact, the USD 2.3-billion investments to modernize the grid include utilizing distributed energy resources as a key pillar to enhance resilience (White House 2022). For example, rooftop solar panels and behind-the-meter batteries together can provide continuous energy to communities in an outage in the main grid (Ceferino et al. 2020a; Patel et al. 2021). Despite these opportunities, little is known about the ability of panels to generate electricity during hurricanes.

Extensive energy system models can assess disruptions in power systems (Anderson et al. 2018; Colson et al. 2011; Laws et al. 2018; Arora and Ceferino 2023), enabling the design of strategies for risk mitigation (e.g., grid hardening) or emergency response (e.g., grid operations and repairs) (Bennett et al. 2021; Ceferino et al. 2020b; Guikema et al. 2010; Han et al. 2009; Nateghi et al. 2014; Ouyang et al. 2012; Shashaani et al. 2018; Talebiyan and Duenas-Osorio 2020; Winkler et al. 2010). Nevertheless, these studies build on critical assumptions about electricity generation during extreme weather events, especially for solar energy during hurricanes. Many studies focused on damage to the distribution lines, not considering that extreme weather events also damage infrastructure for energy generation (Guikema et al. 2010; Han et al. 2009; Nateghi et al. 2014; Shashaani et al. 2018). Recent observations have shown extensive wind-induced failures in rooftop and ground-mounted panels after Hurricane Irma, Maria, and Dorian in 2017 and 2019 (Burgess et al. 2020; Burgess and Goodman 2018; Stone et al. 2020). Other system models assume that energy sources remain constant during extreme weather events, neglecting transient environmental effects (Bennett et al. 2021; Liu and Zhong 2017; Ouyang et al. 2012; Talebiyan and Duenas-Osorio 2020; Winkler et al. 2010). Yet, hurricanes bring optically-thick clouds that can absorb and reflect light and thus decrease generation drastically, e.g., to a fifth (Cole et al. 2020), during a hurricane emergency (Ceferino et al. 2022).

Current system models cannot capture these effects because no existing quantitative methods take them into account. These effects

[1]Assistant Professor, Dept. of Civil and Urban Engineering, New York Univ., Brooklyn, NY 11201; Assistant Professor, Center for Urban Science and Progress, New York Univ., Brooklyn, NY 11201 (corresponding author). ORCID: https://orcid.org/0000-0003-0322-7510. Email: ceferino@nyu.edu

[2]Associate Professor, Dept. of Civil and Environmental Engineering, Princeton Univ., Princeton, NJ 08540; Associate Professor, Andlinger Center for Energy and the Environment, Princeton Univ., Princeton, NJ 08540.

Note. This manuscript was submitted on September 22, 2022; approved on April 10, 2023; published online on June 19, 2023. Discussion period open until November 19, 2023; separate discussions must be submitted for individual papers. This paper is part of the ***Natural Hazards Review***, © ASCE, ISSN 1527-6988.

are complex because they are compounding and dynamic, i.e., they co-occur with conditions that vary rapidly over a storm's life spans. The DOE, energy regulators, and utility companies must account for these acute effects to assess the risk of solar generation losses and strategize a risk-informed response to outages and an effective deployment of solar energy for grid resilience. Wind hazard maps could provide an initial starting point to identify locations where solar generation infrastructure would be exposed to extreme winds, but there is a lack of formal methods to quantify the risk of solar panel failures and electricity losses during these extreme natural events.

To address this research gap, we present a probabilistic framework to quantify solar generation during hurricanes. This framework integrates recently developed data-driven models to capture the stochasticity in panels' structural performance and the intermittency of solar generation during hurricanes. We first apply the framework to study Miami-Dade, Florida, which faces high hurricane hazards (Vickery et al. 2009) and large-scale hurricane-triggered outages (Mitsova et al. 2019). Then, we extend the study to the 38 central and eastern US states at the county level to elucidate the risk landscape of solar generation. Central and eastern US states are exposed to particularly high wind hazards, especially in coastal areas. Thus, this study allows us to unveil the areas with corresponding high risks and quantitatively determine their extent.

We reveal considerable variability in solar generation risks, highlighting where and when wind-induced panel failures and cloud-driven irradiance reduction are critical. Performing energy system studies to assess the implications of these energy losses on power delivery falls outside this paper's scope. Instead, we apply the proposed methodology to the US to create risk maps of solar generation to help inform the response of utility operators during hurricanes and long-term investments in solar panels for grid resilience.

Materials and Methods

Compounding Solar Energy Losses due to Storms

The dashed line shows solar power and accumulated energy in a nondamaged solar panel during 5 days, i.e., from $t = 0$ to $t = t_f$. The dotted black lines show the counterfactual scenario, energy in the absence of the hurricane, highlighting the reduction in losses from hurricane cloud conditions ΔE_c, represented as the dark-shaded area in Fig. 1(a) and difference between ordinates of the solid and dotted lines in Fig. 1(b). The solid line shows the generation and power for a panel that is damaged at $t = t_d$ due to high hurricane winds. The panel is unable to generate energy after $t = t_d$, generating additional energy losses ΔE_d shown in light-shaded area in Fig. 1(a) and as the difference between ordinates of the dashed and solid lines in Fig. 1(b). Generation will bounce back to normal levels as soon as the hurricane leaves if the panel is undamaged. If the panel is damaged, generation will be zero after $t = t_d$ until it is repaired or replaced. This conceptualization is valid for either small residential rooftop panel arrays or large ground-mounted arrays for utility companies.

We assess the time series of solar generation during hurricanes (Fig. 1). Consider that P is the solar power generation rate during a storm and E is the total harvested energy from a starting time zero of interest (e.g., 24 h before landfall when emergency preparations start) until time t_f in the hurricane emergency. Thus

$$E = \int_0^{t_f} P dt \tag{1}$$

If $\bar{E}$ is the counterfactual energy, i.e., the harvested energy that would have been collected at the same site and time in the absence of the hurricane, then

$$\bar{E} = E + \Delta E_c + \Delta E_d \tag{2}$$

where ΔE_c and ΔE_d = energy losses due to cloud conditions and damage to the panels, respectively. Power generation is first affected by the cloud conditions brought by hurricanes (Ceferino et al. 2023), reducing the irradiance that reaches the panel according to hurricane intensity and proximity. When the hurricane leaves and it is at a sufficient distance away from the site, P will bounce back to normal levels. Thus, ΔE_c is transient. In contrast, if wind conditions are high enough, the panel will be damaged and remain unfunctional, driving power generation P to be permanently 0, starting at $t = t_d$, until the panel is repaired or replaced (Ceferino et al. 2023). Thus, ΔE_d grows indefinitely, and the cumulative electricity generation E will become flat from $t = t_d$. If the panel is repaired or replaced, then ΔE_d will stop increasing because the panel will harvest energy again. However, because our focus is the hurricane emergency, we did not consider this case because this period often lasts only a few days. If there is no failure, ΔE_d will always be zero.

To assess the relative effect of these two factors on the total solar generation, we use two multiplicative factors to characterize solar generation during hurricanes

$$E = \frac{\bar{E}}{A_c A_d} \tag{3}$$

where A_c = reduction factor that accounts for the energy losses due to the optically thick clouds reducing irradiance and is given by

$$A_c = \frac{\bar{E}}{\bar{E} - \Delta E_c} \tag{4}$$

and A_d = reduction factor that accounts for the energy losses due to failures in the solar panel structural system and is given by

$$A_d = \frac{\bar{E} - \Delta E_c}{E} \tag{5}$$

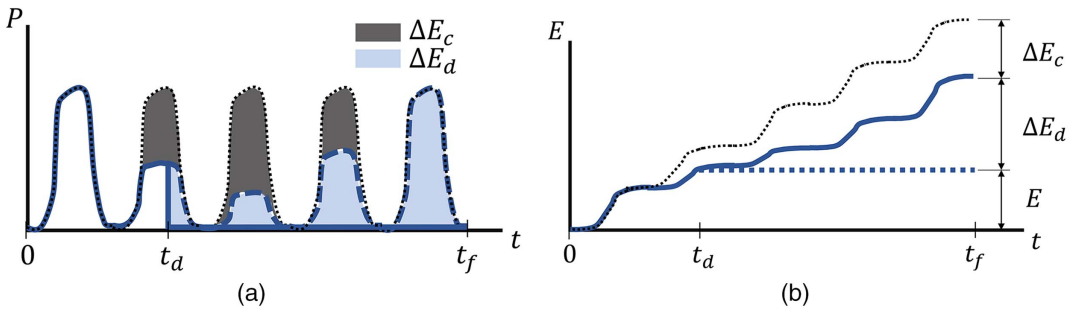

Fig. 1. Conceptual illustration of solar generation losses during hurricanes: (a) instantaneous solar power generation; and (b) cumulative solar energy.

Nat. Hazards Rev., 2023, 24(4): 04023029

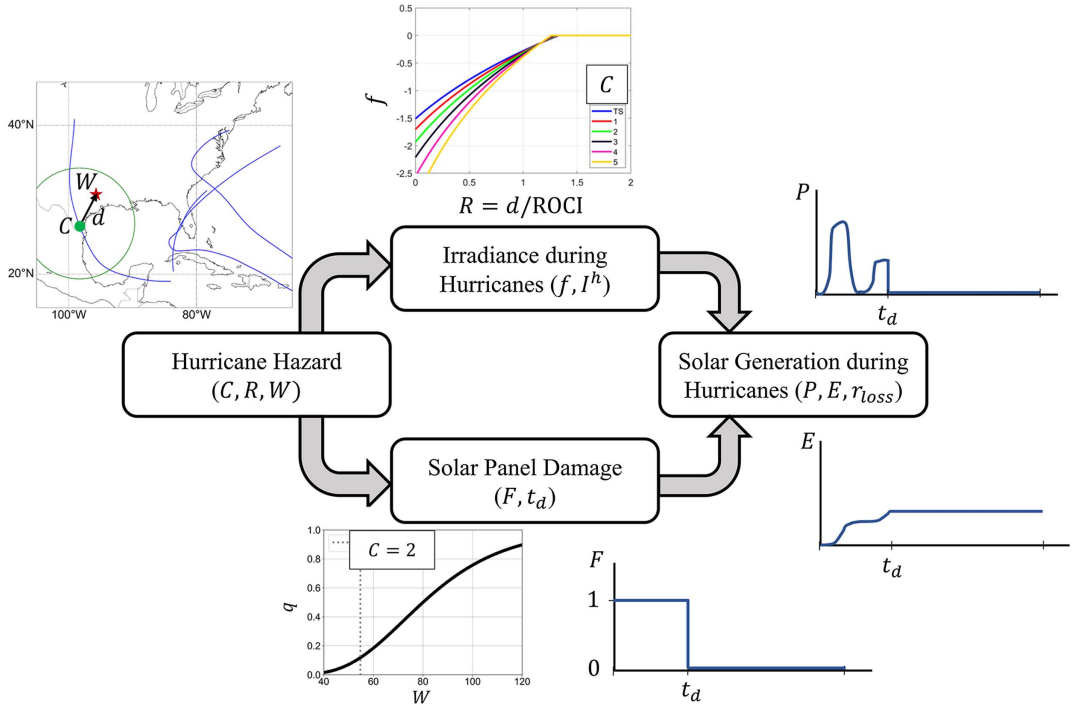

Fig. 2. Overview of proposed probabilistic framework to estimate the times series of solar generation during hurricanes. The analysis builds on the probabilistic modeling of hurricane hazards, solar damage due to high winds, and irradiance decays under hurricane cloud conditions to estimate the resulting solar generation.

Framework for Simulating Time Series of Solar Generation during Storms

To evaluate these compounding effects, we modeled solar generation during storms in four stages (Fig. 2). We based our assessment on ~50,000 Monte Carlo simulations to capture the spatiotemporal complexities in the factors affecting generation. We first used simulations of landfalling synthetic hurricanes representative of the current hurricane climatology in the Atlantic Basin (Marsooli et al. 2019). These simulations of synthetic hurricanes tracked the maximum wind (and thus category, C), storm size, and location of the hurricane's center, which enables the computation of its distance d to any site. This information was modeled at a fine temporal resolution of 2 h, critical to capture intraday variations of solar irradiance and rapid wind intensifications that can damage panels. In the second stage, we assessed solar irradiance during hurricanes (I^h) using a recently developed mixed-regression model (Ceferino et al. 2022). To capture the physics of irradiance decay with hurricanes, this model estimates irradiance decay as a function of hurricane category C and distance d normalized by storm size. In the third stage, solar panel functionality F (1 if there is no structural damage and 0 otherwise) and time-to-damage t_d were estimated stochastically. To account for these impacts on the panels' structural system, we used Ceferino et al.'s (2023) study to link the likelihood of panel damage to varying winds (W) in hurricanes. We further detail Stage 1, 2, and 3's models in the following subsections. In the fourth stage, we used I^h, F, and t_d to compute the synthetic time series of instantaneous solar generation P and cumulative energy E.

For a panel, with efficiency η (the ratio of energy that is converted into electricity form the solar energy reaching the panel) and area a, the instantaneous solar generation is

$$P = FI^h a\eta \tag{6}$$

If we isolate the effect of hurricane clouds (not considering panel failure), then $F = 1$ and

$$P = I_h a\eta \tag{7}$$

Additionally, in regular conditions

$$\bar{P} = Ia\eta \tag{8}$$

where I = irradiance in the absence of a hurricane. Thus

$$\Delta E_c = a\eta \int_0^{t_f} (I - I^h)dt \tag{9}$$

We then estimate our metrics for compounding effects reducing solar generation through the factors A_c and A_d. From Eq. (4)

$$A_c = \frac{a\eta \int_0^{t_f} Idt}{a\eta \int_0^{t_f} Idt - a\eta \int_0^{t_f} (I - I^h)dt} = \frac{\int_0^{t_f} Idt}{\int_{t_0}^{t_f} I^h dt} \tag{10}$$

Similarly, from Eq. (5)

$$A_d = \frac{a\eta \int_0^{t_f} Idt - a\eta \int_0^{t_f} (I - I^h)dt}{a\eta \int_0^{t_f} FI^h dt} = \frac{\int_0^{t_f} I^h dt}{\int_0^{t_f} FI^h dt} = \frac{\int_0^{t_f} I^h dt}{\int_0^{\min(t_d, t_f)} I^h dt} \tag{11}$$

Limiting Behavior of Compounding Factors

Using L' Hospital's rule for the limiting behavior of A_c, then

$$\lim_{t_f \to \infty} A_c = \frac{\int_0^{t_f} Idt}{\int_{t_0}^{t_f} I^h dt} = \lim_{t_f \to \infty} \frac{I}{I^h} \tag{12}$$

Because the hurricane eventually leaves or gets dissipated

$$\lim_{t_f \to \infty} I^h = \lim_{t_f \to \infty} I \tag{13}$$

Thus

$$\lim_{t_f \to \infty} A_c = 1 \tag{14}$$

In the case of A_d, if the panel does not fail, then $F = 1$, and $t_d = \infty$. Thus

$$A_d = \frac{\int_0^{t_f} I^h dt}{\int_0^{t_f} I^h dt} = 1 \tag{15}$$

If the panel fails, $t_d < \infty$ and

$$\lim_{t_f \to \infty} A_d = \frac{\lim_{t_f \to \infty} \int_0^{t_f} I^h dt}{\int_0^{t_d} I^h dt} = \infty \tag{16}$$

Solar Irradiance during Storms

I^h is the irradiance, e.g., global horizontal irradiance, during hurricane conditions and can be estimated as follows:

$$I^h = I e^{f(R,C)} \tag{17}$$

where I = irradiance under normal conditions, i.e., without a hurricane, at the time and location of interest; and $f(R, C)$ = irradiance decay equation as a function of the normalized proximity from the site to the hurricane center R and hurricane intensity C (Fig. 3). According to Ceferino et al. (2022), this factor can be assessed as follows:

$$f = \begin{cases} (0.0965C + 1.97) \ln\left(\dfrac{R + (-0.126C + 1.15)}{2.48\text{–}0.139C}\right) & \dfrac{R + (1.15\text{–}0.126C)}{2.48\text{–}0.139C} \le 1 \\ 1 & \dfrac{R + (1.15\text{–}0.126C)}{2.48\text{–}0.139C} > 1 \end{cases} \tag{18}$$

where C = hurricane intensity in the Saffir-Simpson wind scale; and R = distance from the site of interest to the hurricane center, normalized by the hurricane's radius of the outermost closed isobar (ROCI). ROCI can be estimated from the synthetic storm's radius of maximum wind using an empirical equation (Ceferino et al. 2022). This irradiance model was calibrated to ~0.75 million data points from the 20-years of intense storm activity archived in the Atlantic hurricane data set (HURDAT2) (Landsea and Franklin 2013) and high-resolution spatiotemporal data set of global horizontal irradiance (GHI) from the National Renewable Energy Laboratory (NREL) (Sengupta et al. 2018).

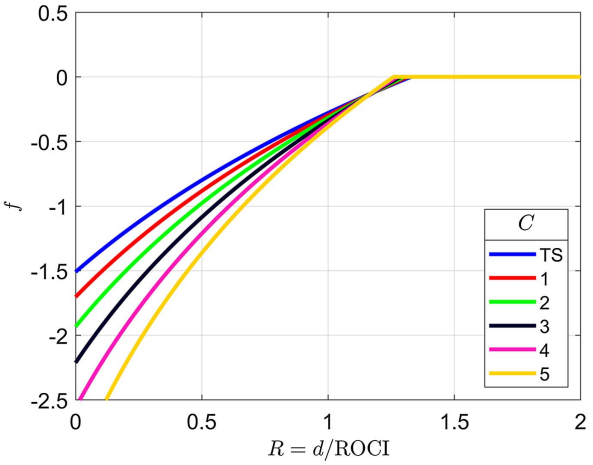

Fig. 3. Functional form (in logarithmic scale) of irradiance decay during hurricanes due to cloud conditions as a function of distance from the site to the storm's center [normalized by the radius of outermost closed isobar (ROCI)] and tropical storm (TS) category in the Saffir-Simpson Scale. R and C are dynamic during the hurricane life span. Plot based Ceferino et al. (2022).

R and C are dynamic over the hurricane life span. As the hurricane approaches the site of interest and potentially strengthens before landfall, f and thus I^h become smaller (Fig. 3). Conversely, as the hurricane leaves and weakens, f and thus I^h increase. Therefore, I^h is highly dynamic. Also, I^h is stochastic as I is random [Eq. (17)]. If we assume I is lognormally distributed, then I^h is also lognormally distributed, with a logarithmic mean that is smaller in f units and a logarithmic standard deviation that is the same to the one for I. Following the procedure of Ceferino et al. (2022), the logarithmic means and standard deviations of I at the site were computed using each county's 20-year history of irradiance (Sengupta et al. 2018). They were then adjusted to sample I^h every 2 h during the life span of each synthetic hurricane.

Damage to Panels during Storms

High hurricane winds increase the likelihood of panels' structural failure and loss of functionality. The functional form of damage likelihood, i.e., fragility function, uses natural hazards' intensities as input, such as maximum wind for hurricanes or spectral acceleration for earthquakes. Accordingly, we utilized the following fragility function recently calibrated (Ceferino et al. 2023) with a ground-truth data on panel structural performance after Hurricane Irma and Maria in 2017 and Dorian in 2019 (Burgess et al. 2020; Burgess and Goodman 2018; Stone et al. 2020):

$$q = \Phi\left(\frac{\ln(W) - \ln(80)}{0.32}\right) \tag{19}$$

where q = damage probability; W = 3-s gusts at a site (m/s); and $\Phi(\cdot)$ = cumulative standard normal distribution function. The data set consisted of observations of damages in 46 rooftop solar panel installations in the Caribbean. Failure modes included clip (clamp), racking, and roof attachment failures on rooftop panels, especially for panels that experienced strong winds. Fig. 4 shows the calibrated fragility function for multiple values of W. Damage is only caused

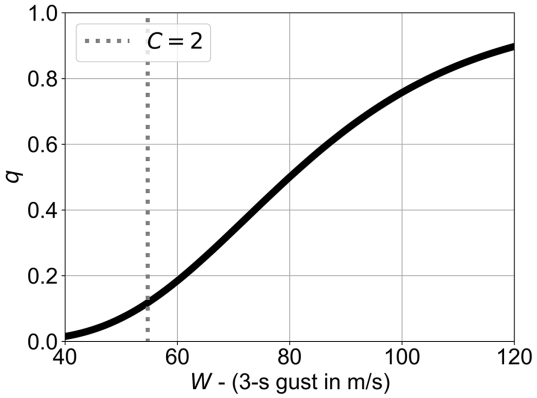

Fig. 4. Fragility functions for solar panels fitted to solar panel damage after Hurricanes Irma and Maria in 2017 and Dorian in 2019 in the Caribbean. The fitting was conducted in a previous study using a Bayesian approach, and in this study, we used the maximum a posteriori estimates from the parameter joint distribution based on Ceferino et al. (2023). For reference, 3-s winds for a Category 2 hurricanes are included based on Vickery and Skerlj (2005) to highlight that storms with lower intensity will have low chances of damaging panels.

by high-intensity hurricanes. For hurricanes reaching Category 1, W is 42 m/s [after transforming 1-m sustained winds to 3-s gusts with an empirical formula (Vickery and Skerlj 2005)], and q is only 0.02. It takes an intensity of Category 4 ($W = 74$ m/s) to increase the probability of failure to 0.4. In our model, $F = 1$ until t_d and = 0 after. If the panel is undamaged, then the time to failure $t_d = \infty$. Thus, $t_d = \infty$ with probability of $1 - q_{\max}$, where $q_{\max}$ is the maximum q induced at the site of interest during the life span of the hurricane. Conversely, $t_d < \infty$, i.e., there is a failure, with probability of $q_{\max}$.

We modeled the time to failure stochastically, with probability of failure at time t proportional to the varying values of q during the hurricane's life span. Although high-resolution and high-fidelity structural analysis models may better capture t_d, this simplified approach accounts for the fact that it is more likely to have failures during the highest wind conditions imposed by hurricanes.

Hurricane Simulation

We used a synthetic hurricane database with 5018 landfalling storms in the US Atlantic Coast, and simulated 10 time series of solar generation for each storm, reaching ~50,000 simulations. The synthetic hurricanes were generated in a previous study (Marsooli et al. 2019) using a statistical-deterministic tropical cyclone model. These synthetic hurricanes account for current climate conditions, representative of hurricane activity from 1980 to 2005 according to the National Center for Environmental Prediction (NCEP) reanalysis. The model that generates these storms consists of three stages: a probabilistic genesis model, a probabilistic beta-advection motion model, and a deterministic model that captures how environmental factors influence the development of storm intensity (Emanuel et al. 2008). The model solves the synthetic storms' tracks, maximum sustained winds, and radii of maximum winds, and we use its results at 2-h intervals.

We estimated the total wind fields with a complete wind profile model (Chavas et al. 2015) and estimated background winds (Lin and Chavas 2012). The average rate of landfalling tropical cyclones in the US Atlantic coast from 1980 to 2005 was 3.37 per year (Landsea and Franklin 2013). Accordingly, the total ~50,000 simulations are representative of ~14,850 years of simulation of solar generation during storms, i.e., to match the rates of historical and synthetic tropical cyclones.

Results and Discussion

We studied the impact of a large number of synthetic storms (Marsooli et al. 2019) making landfall on the US Atlantic Coast. The storm simulations account for current climate conditions and include the assessment of the synthetic storms' track, size, and wind field at 2-h intervals. We determined solar generation reduction factors A_c and A_d at this high temporal resolution to capture intermittency of solar generation within a day and its seasonal variability during storms, which occur at different monthly rates (Emanuel 2006).

To capture different risk levels, we used our probabilistic approach to estimate the return period (RP) for the total reduction factor, A_cA_d, as the inverse of its annual exceedance rate λ. Using the n Monte Carlo simulations, we computed the empirical estimate of this rate as follows:

$$\hat{\lambda}(A_cA_d > x) = \frac{\sum_{i=1}^{n} 1\{A_c^i A_d^i > x\}}{T} \tag{20}$$

where x = threshold of interest. The summation computes the number of simulations (with index i) that exceed the threshold, and T is the equivalent number of years of simulation. We followed a similar procedure to calculate the RP for A_c and A_d.

Risk of Solar Generation in Miami-Dade

We utilized our proposed framework to first generate ~50,000 Monte Carlo simulations of the time series of P and E in Miami-Dade, Florida (Fig. 5). We characterized the occurrence of energy losses probabilistically, estimating different levels of total reduction factor, i.e., A_cA_d [Eq. (3)], and their associated return periods RP [Eq. (20)]. The total reduction factor was assessed for the total harvested solar energy starting the day before hurricane landfall, i.e., $t = 0$, because important energy losses also occur when the hurricane's center is still on the ocean but near the coastline (Ceferino et al. 2022; Cole et al. 2020).

Our simulations capture how more extreme events (longer RP) trigger larger solar energy losses, i.e., large total reduction factors A_cA_d, across the wide range of return periods at landfall and 1 day ($t_f = 24$ h), 2 days ($t_f = 48$ h), and 3 days ($t_f = 96$ h) days after [Fig. 6(a)]. We also show that even frequent events will induce large energy generation losses, with total reduction factors increasing sharply in the initial return period range. Miami-Dade will lose 70%, 63%, 52%, and 40% of its solar generation, i.e., $A_cA_d = 3.3$, 2.7, 2.1, and 1.67, at landfall and 1, 2, and 3 days after, respectively, for hurricane emergencies happening on average every 50 years (RP = 50 years).

Time-Variant Contributions of Reduction Factors

We observed that the total reduction factor was bigger at landfall than 3 days after for the frequent events [Fig. 6(a)]. However, they reached similar values, A_cA_d of ~3.4, for hurricanes with RP of ~90 years. For rarer events, the order flips, and energy losses increased over time after landfall in Miami-Dade due to the varying contributions of the factors A_c and A_d through the wide range of

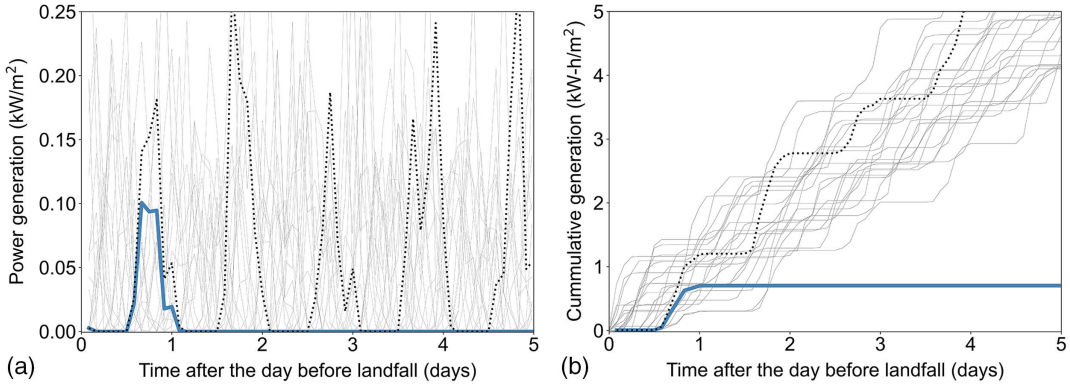

Fig. 5. Multiple simulations of solar generation in Miami-Dade, Florida, for future tropical storms in thin gray lines: (a) Instantaneous power generation (P); and (b) Cumulative solar energy (E). The synthetic simulations of solar generation start at one day before landfall ($t = 0$). The contrast between thicker solid line and dotted line highlights the difference between solar power (P) and generation (E) during the storm (in solid line) and under the counterfactual power (P) and generation (E) if there would have not been a hurricane (in dotted lines). P is reduced due to hurricane clouds and it becomes 0 if the panel has structural failure. E becomes flat after the panel's failure.

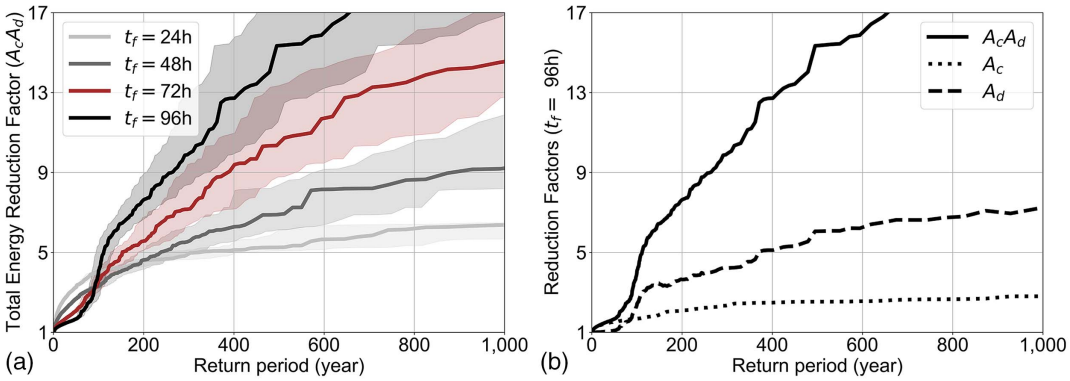

Fig. 6. Return periods for different levels of relative energy loss due to hurricanes for Miami-Dade, Florida: (a) relative energy loss is depicted through total reduction factors, A_cA_d, equal to the cumulative energy harvested by the panel until landfall and 1, 2, and 3 days after ($t_f = 24$, 48, 72, and 96 h) compared with the counterfactual event, i.e., generation in the absence of a hurricane; 95% confidence was estimated using χ^2 distributions for Poisson rate estimates (Ulm 1990) and are shown as shaded areas; and (b) total reduction factor is decomposed in its two factors, A_c and A_d, for cumulative energy until 72 h after landfall ($t_f = 96$ h) to highlight the contributions of cloud conditions and panel damage in the energy losses for different return periods.

return periods [Fig. 6(b)]. A_c was initially bigger than A_d until they reached a similar value of 1.7 for a RP of ~90 years for $t_f = 96$ h. This RP threshold coincides with the transition from decreasing to increasing values of A_cA_d as a function of t_f. Empirically, we demonstrate that this transition is dominated by the change in the energy loss mode, from predominantly transient and cloud-induced to permanent and damage-induced losses.

We also observed transient but strong cloud-induced energy losses, especially for small t_f. For example, at $t_f = 6$ h, i.e., 18 h before landfall, events with RP of 200 years will trigger losses of 68% [Fig. 7(a)], almost entirely due to the hurricane clouds ($A_c = 3.1$ and $A_d = \sim 1$). Cloud-induced losses will reach their maximum values of 77% ($A_c = 4.4$) for $24 < t_f < 36$ h (between landfall and the 12 h after). This observation is consistent with presence of optically thick cloud structures (with high moisture levels and vertical depths) in the hurricane eyewalls (John et al. 2020) that will cover Miami-Dade after landfall. More frequent events can also induce large energy losses. In events with RP of only 9 years, clouds will induce losses of 50% ($A_c = 2$) at $t_f = 6$ h. These strong cloud effects are transient. Thirteen days after landfall, A_c is only 1.19 with return period of 200 years, which is a modest energy loss of 11% for an extreme event [Fig. 7(a). As time goes on, cloud-induced losses will be negligible, i.e., $A_c = 1$ in the limit [Eq. (14)].

Less frequent events (RP > ~90 years) can have permanent effects on energy [Fig. 7(b)]. A_d is close to 1 for RP < ~90 years for all values of t_f, and then it grows steadily as a function of the return period given that these extreme events will induce higher solar panel damage likelihoods (Fig. 4). In contrast to A_c, A_d is close to 1 (below 1.03), i.e., no effects, until $t_f = 36$ h (12 h after landfall) even for very extreme events with RP of 1,000 years, demonstrating that storms require additional time to be near the site and damage panels. If the panel is damaged, then energy losses will grow to infinite unless the panel is repaired or replaced [Eq. (16)]. Accordingly, the factor A_d becomes rapidly dominant for damaged panels. For events with RP of 200 years, the ratio between A_d and A_c is 0.4 at $t_f = 48$ h, but it increases to 1.8 only 48 h after (Fig. 7).

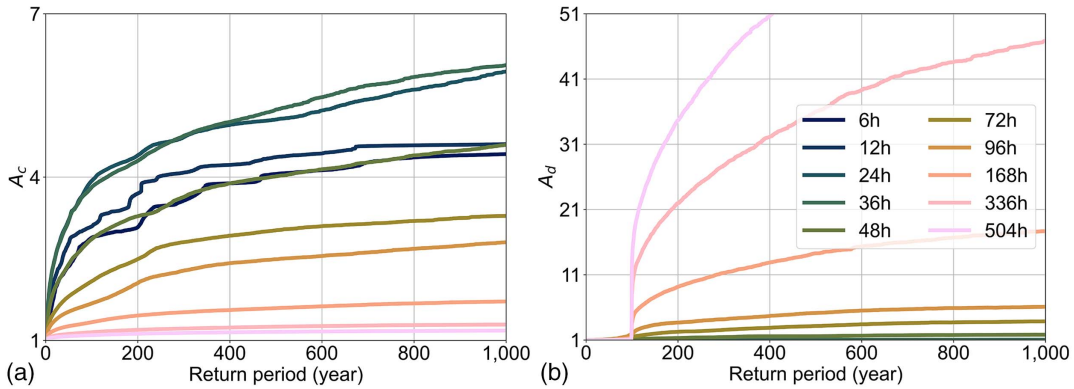

Fig. 7. Time-varying behavior of compounding factors A_c and A_d across different return periods: (a) reduction factor due to cloud conditions (A_c); and (b) reduction factor due to solar panel damage (A_d). The reduction factors were estimated for cumulative energy losses starting at 24 h before landfall until different t_f values, i.e., the values of A_c and A_d for $t_f = 6$ h correspond to cumulative from 24 h before landfall until 18 h before landfall.

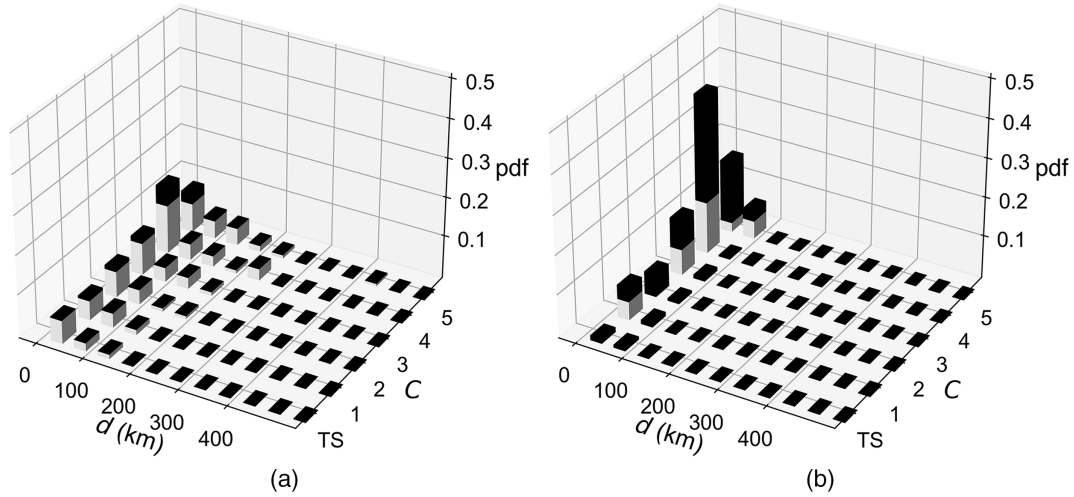

Fig. 8. Analysis of the drivers of energy capacity loss through deaggregation of the simulations for Miami-Dade, Florida: (a) $A_cA_d = 1.3$ ($A_c = 1.29$, $A_d = 1.01$, and RP = 12 years); and (b) $A_cA_d = 2$ $A_c = 1.59$, $A_d = 1.26$, and RP = 58 years). The plots show histograms of the storms' features that triggered generation losses of 33 and 50%, respectively, or lower. The dark-shaded portion of the plot represents losses associated to structural failures, and the light-shaded portion represents losses due to hurricane clouds. The plots highlight that larger capacity losses are driven by structural failures rather than hurricane cloud conditions.

These results demonstrate that structural reliability is critical for generation reliability during a hurricane emergency.

Storms' Features Driving Bigger Energy Losses

We deaggregated the storm simulations to assess the storm features driving large energy losses quantitatively. We analyzed the joint probability distribution of category C and distance to the site d, empirically, utilizing 500,000 Monte Carlo simulations (by simulating 100 time series of solar generation for each synthetic storm) instead of 50,000 to estimate these joint distributions more smoothly. We analyzed the drivers for energy losses of 33% and 50%, i.e., A_cA_d of 1.3 (RP of 12 years) and 2 (RP of 58 years), at $t_f = 96$ h (Fig. 8). The average hurricane categories that caused these losses were 3.1 and 3.6, and the average closest distances were 66 and 33 km, respectively. Hurricane cloud conditions rather than high winds drove the reduction factor of 1.3 because 88% of the storms did not cause panel failure; 33% of these synthetic storms did not reach hurricane categories beyond Category 2, and 44% were more than 50 km away, indicating that the 1.3 reduction factor can be caused by events distant from the site. For the reduction factor of 2, panels experienced failures in 69% of the simulations, indicating that significant panel damage can occur at return periods of A_cA_d lower than 90 years (although panel damage can only occur at return period of A_c greater than 90 years [Fig. 7(b)]. Moreover, 72% of the simulations had storms with categories above Category 3, and 90% had distances from the track to the site of 50 km or less. This result is consistent with frequent observations of hurricane's maximum winds at radii between 20 and 80 km (Wang and Rosowsky 2012).

Annual Rates of Panel Failure in Central and Eastern US

We extended the analysis to the entire central and eastern US and generated 50,000 Monte Carlo simulations for their 2,694 counties in 38 states. We first focused on simulations of structural damage to assess the spatial distribution of RP and reliability indexes of panel failures. As defined in the ASCE 7-16 (ASCE 2017), the reliability index β was estimated as the cumulative distribution function for

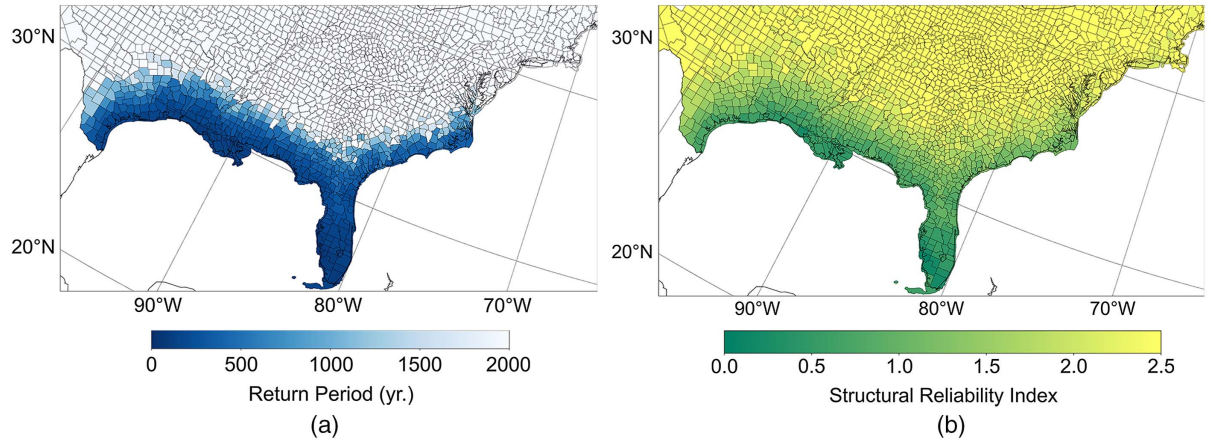

Fig. 9. Spatial distribution of return period of structural failure and reliability index for solar panels located on different counties in the central and eastern US: (a) return period; and (b) structural reliability index. The plot highlights that southern US states have significantly lower reliability than the threshold.

a standard normal random variable evaluated on the probability of infrastructure survival (the complementary of failure) in 50 years. Thus

$$\beta = \Phi^{-1}(\exp(-50\lambda_f)) \tag{21}$$

where λ_f = annual probability of panel failure, equal to the inverse of RP of structural failure. We estimated λ_f empirically from the 50,000 Monte Carlo simulations in the 38 states, like in a maximum likelihood estimation of a Poisson distribution's rate, and then computed RP [Fig. 9(a)] and β [Fig. 9(b)]. We show that Florida and Louisiana face the highest failure risks due to hurricanes, with average RP of 174 years and 265 years across all their counties; 55% and 41% of the counties in Florida and Louisiana have RP of panel failure below 200 years. Our results also show that Texas, Mississippi, Alabama, Georgia, and South and North Carolina also have high risks, where installed solar panels will experience failures with RP below 600 years in 19%, 22%, 19%, 26%, 24%, and 12% of their counties, respectively.

Using results from a recent reliability study that assessed wind loads and capacities according to ASCE 7-16 (McAllister et al. 2018), we estimated that a structure well designed for Risk category II (winds with a 700-year return period) should have a β at or above 2.3 (ASCE 2017). For the Risk category I (winds with a 300-year return period), the lowest design standard in ASCE7-16, a well-designed structure should achieve a β value at or above 1.9 (ASCE 2017; Ceferino et al. 2023; McAllister et al. 2018). Our results indicate that the panel installations in Texas, Louisiana, Mississippi, Alabama, Florida, Georgia, and South and North Carolina have β values below 1.9 in 62% of their counties. Thus, these results reveal extensive structural vulnerabilities and highlight that panels are below all ASCE 7-16 standards for resilience in large regions in the southern US [Fig. 9(b)].

Spatial Distribution of Solar Generation Losses in Central and Eastern US

Next, we assessed generation during storms in the central and eastern US. We generated 50,000 Monte Carlo simulations of the time series of P and E for panels in the 2,694 counties' centroids (the examples of Texas and North Carolina are shown in Fig. S1). Similar to the analysis in Miami-Dade, we determined the reduction factors A_c and A_d at different return periods. We assessed return periods of 100, 300, and 700 years to evaluate a wide range of extreme events. Solar panels might not have a high probability of experiencing energy losses with 700-year return periods because their life span is ~30 years. However, it is critical to understand how they behave under these extreme conditions, especially under warming climates that can intensify tropical cyclones. Furthermore, as stated previously, the ASCE 7-16 standards require us to design infrastructure for wind levels associated with long return periods, e.g., from 300 to 3,000. Thus, we assessed here how these rare events affect solar generation. We focused on cumulative energy at t_f = 24 h (Fig. 10), 48 h (Fig. S2), 72 h (Fig. 11), and 96 h (Fig. S3).

The spatial distribution of A_c at $t_f = 24$ h revealed that hurricane clouds will induce significant energy losses at landfall even at tens of kilometers away from the southern and eastern US coastline (Fig. 10). For a RP of 100 years, Florida and Louisiana will only harvest 32% ($A_c = 3.13$) and 65% ($A_c = 1.54$) of their regular solar energy on average across all their counties, with hardest-hit counties generating only at 23% ($A_c = 4.27$) and 27% ($A_c = 3.65$), respectively. More extreme events will increase the intensity and the spatial extent of high energy losses. For RP of 300 years, Florida and Louisiana will only harvest 21% ($A_c = 4.80$) and 50% ($A_c = 2.01$) on average across all their counties. For RP of 700 years, they will only harvest 25% ($A_c = 4$) and 54% ($A_c = 1.84$), with hardest-hit counties generating only at 17% ($A_c = 5.83$) and 18% ($A_c = 5.46$) of regular capacity, respectively. All southern and central counties near the coastline up to the ones in Virginia, Maryland, and Delaware will have reduced generation equal or below 33% due to the storm clouds ($A_c > \sim 3$).

Our results showed that compounding effects will be critical only after $t_f = 24$ h, i.e., at landfall. Before, $A_c A_d$ is almost equivalent to A_c across the different levels of storms' return periods for all counties (Fig. 10). However, at $t_f = 72$ h (2 days after landfall), we started observing important contributions of solar damage to the energy losses (Fig. 11). At this time, Florida and Louisiana already experienced 26% and 15% less energy losses than at landfall, thanks to the recovery of regular irradiance levels after the hurricane leaves, but damage-induced losses will start dominating the total energy losses. In counties on the coastline, this transition can happen as early as 24 h after landfall (Fig. S2).

For RP of 300 years, A_d across all of Florida and Louisiana's counties was 2.03 and 1.13 at $t_f = 72$ h (2 days after landfall), inducing energy losses 25% and 9% higher than those when panels do not fail, respectively. For RP of 700 years, the compounding effect of damage becomes stronger because A_d increases to 3.48

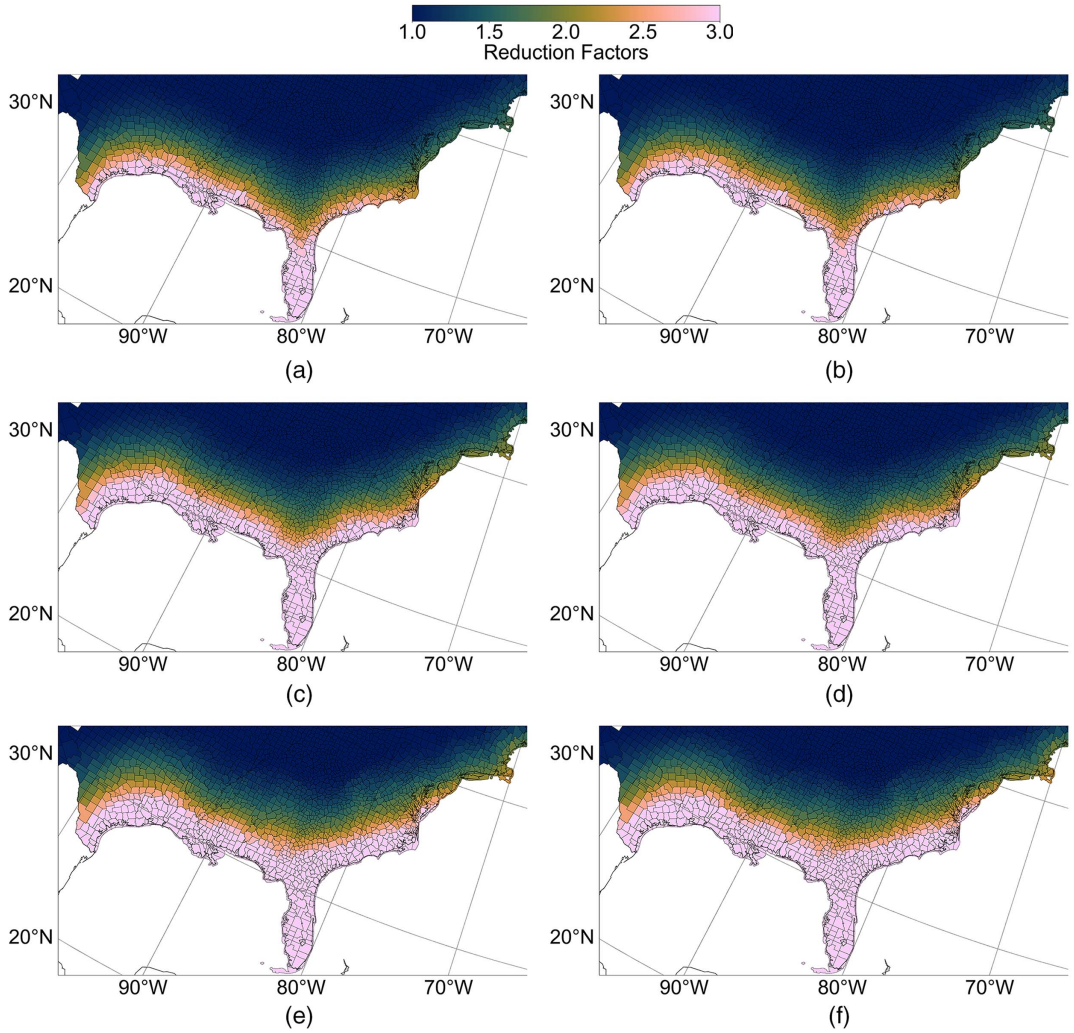

Fig. 10. Spatial distribution of energy generation losses for uniform risk targets (associated to return periods) in the central and eastern US and the compounding factors for energy losses at landfall ($t_f = 24$ h): (a) A_c for events with a 100-year return period; (b) A_cA_d for events with a 100-year return period; (c) A_c for events with 300-year return period; (d) A_cA_d for events with a 300-year return period; (e) A_c for events with a 700-year return period; and (f) A_cA_d for events with a 700-year return period.

and 1.39 for Florida and Louisiana, respectively, inducing 38% and 25% higher losses, which will become even stronger for longer t_f (Fig. 11).

Limitations and Future Research

This study focused on understanding the resilience of solar generation during hurricanes. As such, it quantified how much electricity can be harvested from solar panel installations during storms. However, it did not evaluate whether a grid with solar farms will become more resilient or if customers with rooftop panels will access sufficient electricity. Understanding the grid's resilience and household access to electricity requires modeling households and critical infrastructure's demands for electricity during a hurricane, which can be quite different from normal conditions. Further, assessing grid resilience also requires the assessment of power flow through potentially vulnerable transmission and distribution lines that can disrupt solar electricity delivery. To fill these research gaps, future research could integrate models for solar generation, like the one presented in this paper, with models representing power demands during disasters and network models capturing power system behavior to holistically quantify power system resilience.

Discussion

In sum, our results show that hurricane's impacts on solar generation are significant, compounding and strikingly disproportional in the US. Clouds can induce losses above 66% in extensive regions in the southern and eastern US (e.g., RP of 100 years in Fig. 10), but fortunately, these effects are only transient. In contrast, damage to solar panels will induce more acute and permanent energy losses but fortunately in smaller extents (e.g., counties with highest risk of panel failure in Fig. 9). When these two effects are compounded, solar generation risk will induce large energy losses throughout the entire hurricane emergency.

A direct implication of this study is that the naïve adoption of panels in the current conditions will create electricity generating infrastructure with high risks, especially in Louisiana and Florida, which have experienced massive hurricane outages in the last few years (Boyle 2021; Esnard 2018; Prevatt et al. 2021). Building stronger panels can help prevent panel damage, i.e., making $A_d = 1$. Thus, this paper advocates installing stronger panels, at least up to the ASCE-7 standards for infrastructure with Risk category I. Existing studies pointed out that cheap solutions can increase the performance of solar installation's structural system, e.g., torque

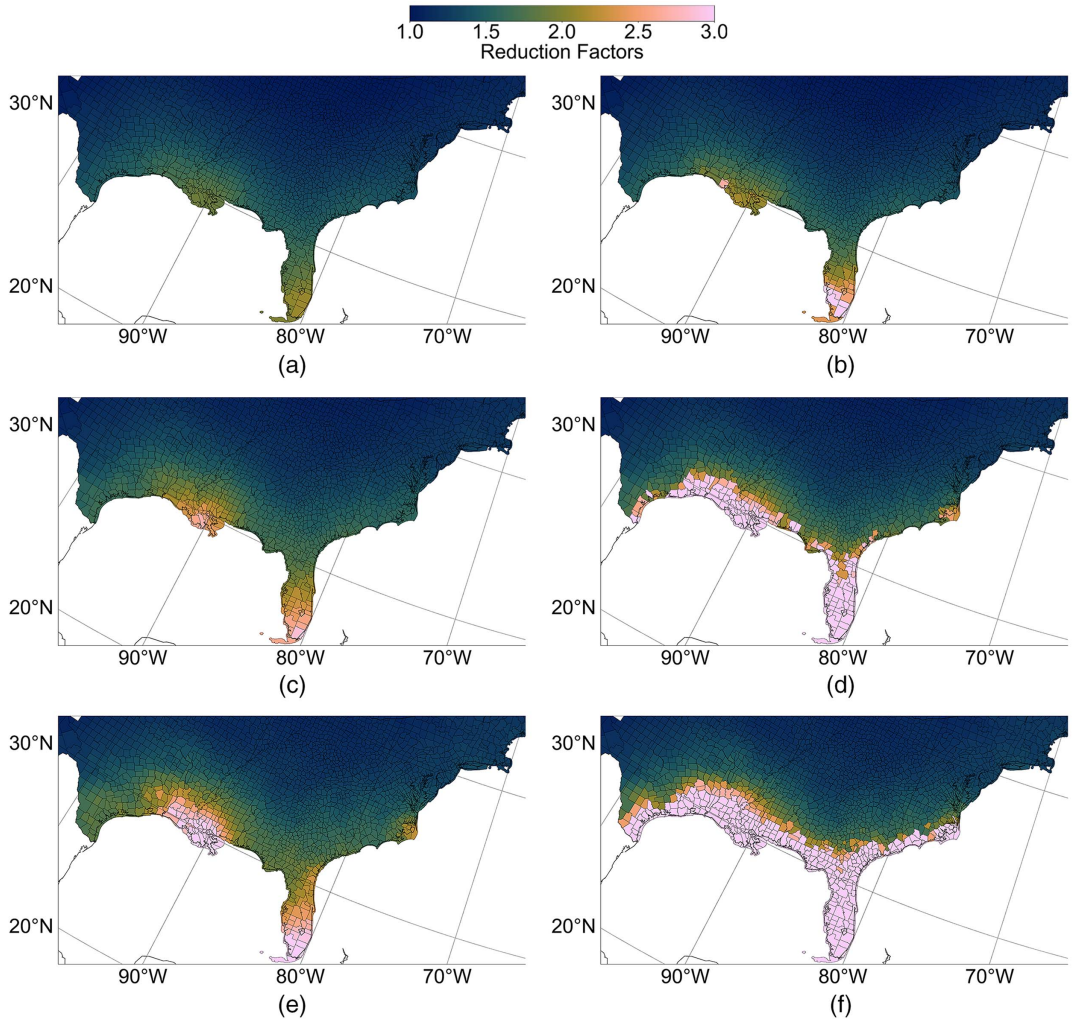

Fig. 11. Spatial distribution of energy generation losses for uniform risk targets (associated to return periods) in the central and eastern US and the compounding factors for energy losses 48 h after landfall ($t_f = 72$ h): (a) A_c for events with a 100-year return period; (b) A_cA_d for events with a 100-year return period; (c) A_c for events with a 300-year return period; (d) A_cA_d for events with a 300-yearreturn period; (e) A_c for events with a 700-year return period; and (f) A_cA_d for events with a 700-year return period.

check on bolts (Burgess et al. 2020; Burgess and Goodman 2018). If panels do not fail, all solar energy reductions (A_c) will be driven by hurricane clouds only, making solar energy losses only transient.

These results underscore that massive investments in resilience and clean energy in power infrastructure will pay off if their deployment is risk-informed. Placing panels on coastlines in the southern or eastern US can make the grid lose (sometimes permanently) solar generation during hurricane emergencies (Figs. 10 and 11). Power system models can optimize the deployment of new solar farms, maximizing profits for regulators, power utility companies, and consumers. But they should also assess resilience to consider the trade-off between costs and risks, especially in Florida and Louisiana, where generation potential is high, but risks are also high.

Additionally, for communities exposed to high risks, like those in Miami-Dade or New Orleans installing decentralized resources, such as rooftop panels and behind-the-meter batteries must account for the potential high reduction in energy generation. Even if they have continuous power supply even in case of a main grid's outage, they should still plan for only using necessary building functions in a hurricane emergency, e.g., refrigeration for food or even cooling, especially if heatwaves follow storms (Feng et al. 2022).

This paper also advocates risk-informed utility companies' contingency planning during extreme events. We provide a framework to account for these losses quantitatively so that utility companies can plan for offsetting the large losses in solar generation from other sources. In the context of disaster, additional difficulties might arise from failures in transmission lines that prevent the use of other functional electricity sources. Thus, it is critical for utility companies to install robust generating infrastructure to ensure the resilience of our future grids, especially because global warming is projected to intensify hurricanes in the future climate (Knutson et al. 2020).

Data Availability Statement

All data, models, or code that support the findings of this study are available from the corresponding author upon reasonable request.

Acknowledgments

We acknowledge the financial support by the Tandon School of Engineering at the New York University and the Andlinger Center

for Energy and the Environment at Princeton University. Additionally, this research was also supported by the NSF Grant 1652448. The authors are grateful for their generous support. We also thank Dr. Dazhi Xi, from Princeton University, for his help in generating the wind fields and Dr. Charalampos Avraam, from New York University, for his insightful comments and revisions to our study's contributions for power systems resilience.

Supplemental Materials

Figs. S1–S3 are available online in the ASCE Library (www.ascelibrary.org).

References

Anderson, K., N. D. Laws, S. Marr, L. Lisell, T. Jimenez, T. Case, X. Li, D. Lohmann, and D. Cutler. 2018. "Quantifying and monetizing renewable energy resiliency." *Sustainability* 10 (4): 1–13. https://doi.org/10.3390/su10040933.

Arora, P., and L. Ceferino. 2023. "Probabilistic and machine learning methods for uncertainty quantification in power outage prediction due to extreme events." *Nat. Hazards Earth Syst. Sci.* 23 (5): 1665–1683. https://doi.org/10.5194/nhess-23-1665-2023.

ASCE. 2017. *Minimum design loads and buildings and other structures*. ASCE/SEI 7-16. Reston, VA: ASCE.

Bennett, J. A., C. N. Trevisan, J. F. DeCarolis, C. Ortiz-García, M. Pérez-Lugo, B. T. Etienne, and A. F. Clarens. 2021. "Extending energy system modelling to include extreme weather risks and application to hurricane events in Puerto Rico." *Nat. Energy* 6 (3): 240–249. https://doi.org/10.1038/s41560-020-00758-6.

Boyle, L. 2021. "Louisiana's power grid took a bigger blow from Hurricane Ida than any other storm in history." Accessed January 1, 2023. https://www.independent.co.uk/climate-change/news/hurricane-ida-power-grid-louisiana-b1915145.html.

Burgess, C., S. Detweiler, C. Needham, and F. Oudheusden. 2020. "Solar under storm Part II: Select best practices for resilient roof-mount PV systems with hurricane exposure." Accessed January 1, 2023. https://rmi.org/solar-under-storm-part-ii-designing-hurricane-resilient-pv-systems/.

Burgess, C., and J. Goodman. 2018. "Solar under storm. Select best practices for resilient ground-mount PV systems with hurricane exposure." Accessed January 1, 2023. https://rmi.org/wp-content/uploads/2018/06/Islands_SolarUnderStorm_Report_digitalJune122018.pdf.

Ceferino, L., N. Lin, and D. Xi. 2022. "Stochastic modeling of solar irradiance during hurricanes." *Stochastic Environ. Res. Risk Assess.* 36 (9): 2681–2693. https://doi.org/10.1007/s00477-021-02154-2.

Ceferino, L., N. Lin, and D. Xi. 2023. "Bayesian updating of solar panel fragility curves and implications of higher panel strength for solar generation resilience." *Reliab. Eng. Syst. Saf.* 229 (Jan): 108896. https://doi.org/10.1016/j.ress.2022.108896.

Ceferino, L., C. Liu, I. Alisjahbana, S. Patel, T. Sun, A. Kiremidjian, and R. Rajagopal. 2020a. "Earthquake resilience of distributed energy resources." In *Proc., 17th World Conf. on Earthquake Engineering*. Sendai, Japan: International Association for Earthquake Engineering.

Ceferino, L., J. Mitrani-Reiser, A. Kiremidjian, G. Deierlein, and C. Bambarén. 2020b. "Effective plans for hospital system response to earthquake emergencies." *Nat. Commun.* 11 (1): 4325. https://doi.org/10.1038/s41467-020-18072-w.

Chavas, D. R., N. Lin, and K. Emanuel. 2015. "A model for the complete radial structure of the tropical cyclone wind field. Part I: Comparison with observed structure." *J. Atmos. Sci.* 72 (9): 3647–3662. https://doi.org/10.1175/JAS-D-15-0014.1.

Cole, W., D. Greer, and K. Lamb. 2020. "The potential for using local PV to meet critical loads during hurricanes." *Sol. Energy* 205 (Jul): 37–43. https://doi.org/10.1016/j.solener.2020.04.094.

Colson, C. M., M. H. Nehrir, and R. W. Gunderson. 2011. "Distributed multi-agent microgrids: A decentralized approach to resilient power system self-healing." In *Proc., ISRCS 2011: 4th Int. Symp. on Resilient Control Systems*, 83–88. New York: IEEE. https://doi.org/10.1109/ISRCS.2011.6016094.

Department of Energy. 2022. "DOE optimizes structure to implement $62 billion in clean energy investments from bipartisan infrastructure law." Accessed January 1, 2023. https://www.energy.gov/articles/doe-optimizes-structure-implement-62-billion-clean-energy-investments-bipartisan.

Emanuel, K. 2006. "Climate and tropical cyclone activity: A new model downscaling approach." *J. Clim.* 19 (19): 4797–4802. https://doi.org/10.1175/JCLI3908.1.

Emanuel, K., R. Sundararajan, and J. Williams. 2008. "Hurricanes and global warming: Results from downscaling IPCC AR4 simulations." *Bull. Am. Meteorol. Soc.* 89 (3): 347–368. https://doi.org/10.1175/BAMS-89-3-347.

Esnard, D. M. A. 2018. "Socioeconomic vulnerability and electric power restoration timelines in Florida: The case of Hurricane Irma." *Nat. Hazards* 94 (2): 689–709. https://doi.org/10.1007/s11069-018-3413-x.

Feng, K., M. Ouyang, and N. Lin. 2022. "Tropical cyclone-blackout-heatwave compound hazard resilience in a changing climate." *Nat. Commun.* 13 (Jul): 4421. https://doi.org/10.1038/s41467-022-32018-4.

Guikema, S. D., S. M. Quiring, and S. R. Han. 2010. "Prestorm estimation of hurricane damage to electric power distribution systems." *Risk Anal.* 30 (12): 1744–1752. https://doi.org/10.1111/j.1539-6924.2010.01510.x.

Han, S. R., S. D. Guikema, and S. M. Quiring. 2009. "Improving the predictive accuracy of hurricane power outage forecasts using generalized additive models." *Risk Anal.* 29 (10): 1443–1453. https://doi.org/10.1111/j.1539-6924.2009.01280.x.

John, J., B. P. Shukla, P. N. Gajjar, and V. Sathiyamoorthy. 2020. "Study of satellite-derived cloud microphysical parameters for tropical cyclones over the North Indian Ocean (2010–2013)." *Theor. Appl. Climatol.* 139 (3–4): 1163–1173. https://doi.org/10.1007/s00704-019-03047-9.

Knutson, T., et al. 2020. "Tropical cyclones and climate change assessment part II: Projected response to anthropogenic warming." *Bull. Am. Meteorol. Soc.* 101 (3): E303–E322. https://doi.org/10.1175/BAMS-D-18-0194.1.

Landsea, C. W., and J. L. Franklin. 2013. "Atlantic hurricane database uncertainty and presentation of a new database format." *Mon. Weather Rev.* 141 (10): 3576–3592. https://doi.org/10.1175/MWR-D-12-00254.1.

Laws, N. D., K. Anderson, N. A. DiOrio, X. Li, and J. McLaren. 2018. "Impacts of valuing resilience on cost-optimal PV and storage systems for commercial buildings." *Renewable Energy* 127 (Nov): 896–909. https://doi.org/10.1016/j.renene.2018.05.011.

Lin, N., and D. Chavas. 2012. "On hurricane parametric wind and applications in storm surge modeling." *J. Geophys. Res. Atmos.* 117 (9): 1–19. https://doi.org/10.1029/2011JD017126.

Liu, Y., and J. Zhong. 2017. "Risk assessment of power systems under extreme weather conditions: A review." In *Proc., 2017 IEEE Manchester PowerTech*, 22–27. New York: IEEE. https://doi.org/10.1109/PTC.2017.7981141.

Marsooli, R., N. Lin, K. Emanuel, and K. Feng. 2019. "Climate change exacerbates hurricane flood hazards along US Atlantic and Gulf Coasts in spatially varying patterns." *Nat. Commun.* 10 (1): 1–9. https://doi.org/10.1038/s41467-019-11755-z.

McAllister, T. P., N. Wang, and B. R. Ellingwood. 2018. "Risk-informed mean recurrence intervals for updated wind maps in ASCE 7-16." *J. Struct. Eng.* 144 (5): 06018001. https://doi.org/10.1061/(ASCE)ST.1943-541X.0002011.

Mitsova, D., M. Escaleras, A. Sapat, A. M. Esnard, and A. J. Lamadrid. 2019. "The effects of infrastructure service disruptions and socioeconomic vulnerability on hurricane recovery." *Sustainability* 11 (2): 516. https://doi.org/10.3390/su11020516.

Nateghi, R., S. Guikema, and S. M. Quiring. 2014. "Power outage estimation for tropical cyclones: Improved accuracy with simpler models." *Risk Anal.* 34 (6): 1069–1078. https://doi.org/10.1111/risa.12131.

Ouyang, M., L. Dueñas-Osorio, and X. Min. 2012. "A three-stage resilience analysis framework for urban infrastructure systems." *Struct. Saf.* 36–37 (May–Jul): 23–31. https://doi.org/10.1016/j.strusafe.2011.12.004.

Patel, S., L. Ceferino, C. Liu, A. Kiremidjian, and R. Rajagopal. 2021. "The disaster resilience value of shared rooftop solar systems in residential

communities." *Earthquake Spectra* 37 (4): 2638–2661. https://doi.org/10.1177/87552930211020020.

Prevatt, D., et al. 2021. *StEER: Hurricane Ida joint preliminary virtual reconnaissance report: Early access reconnaissance report (PVRR-EARR)*. Seattle, WA: DesignSafe-CI. https://doi.org/10.17603/ds2-3pc2-7p82 v1.

Sengupta, M., Y. Xie, A. Lopez, A. Habte, G. Maclaurin, and J. Shelby. 2018. "The national solar radiation data base (NSRDB)." *Renewable Sustainable Energy Rev.* 89 (Jun): 51–60. https://doi.org/10.1016/j.rser.2018.03.003.

Shashaani, S., S. D. Guikema, C. Zhai, J. V. Pino, and S. M. Quiring. 2018. "Multi-stage prediction for zero-inflated hurricane induced power outages." *IEEE Access* 6 (Oct): 62432–62449. https://doi.org/10.1109/ACCESS.2018.2877078.

Stone, L., C. Burgess, and J. Locke. 2020. "Solar under the storm for policymakers: Select best practices for resilient photovoltaic systems for small island developing states." Accessed January 1, 2023. www.rmi.org/insight/solar-under-storm-for-policymakers.

Swiss Re Institute. 2022. *Natural catastrophes in 2021: The floodgates are open (Issue 1)*. Zurich, Switzerland: Swiss Re Institute.

Talebiyan, H., and L. Duenas-Osorio. 2020. "Decentralized decision making for the restoration of interdependent networks." *ASCE-ASME J. Risk Uncertainty Eng. Syst. Part A: Civ. Eng.* 6 (2): 04020012. https://doi.org/10.1061/AJRUA6.0001035.

Ulm, K. 1990. "Simple method to calculate the confidence interval of a standardized mortality ratio (SMR)." *Am. J. Epidemiol.* 131 (2): 373–375. https://doi.org/10.1093/oxfordjournals.aje.a115507.

US Energy Information Administration. 2022. "Annual energy Outlook 2022." Accessed January 1, 2023. https://www.eia.gov/outlooks/aeo/data/browser/#/?id=16-AEO2022&region=0-0&cases=ref2022&start=2020&end=2050&f=A&linechart=ref2022-d011222a.4-16-AEO2022&sourcekey=0;inGW.

Vickery, P., and P. Skerlj. 2005. "Hurricane gust factors revisited." *J. Struct. Eng.* 131 (5): 825–832. https://doi.org/10.1061/(ASCE)0733-9445(2005)131:5(825).

Vickery, P. J., D. Wadhera, L. A. Twisdale, and F. M. Lavelle. 2009. "U.S. hurricane wind speed risk and uncertainty." *J. Struct. Eng.* 135 (3): 301–320. https://doi.org/10.1061/(ASCE)0733-9445(2009)135:3(301).

Wang, Y., and V. D. Rosowsky. 2012. "Joint distribution model for prediction of hurricane wind speed and size." *Struct. Saf.* 35 (Mar): 40–51. https://doi.org/10.1016/j.strusafe.2011.12.001.

Wang, Z., M. O. Román, Q. Sun, A. L. Molthan, L. A. Schultz, and V. L. Kalb. 2018. "Monitoring disaster-related power outages using NASA black marble nighttime light product." In *Proc., ISPRS—Int. Archives of the Photogrammetry, Remote Sensing and Spatial Information Sciences, XLII–3*, 1853–1856. Göttingen, Germany: Copernicus Publications. https://doi.org/10.5194/isprs-archives-XLII-3-1853-2018.

White House. 2022. "President Biden's Bipartisan Infrastructure Law." Accessed January 1, 2023. https://www.whitehouse.gov/bipartisan-infrastructure-law/#:~:text=TheBipartisanInfrastructureLawwilldeliver%2465 billiontohelpinvestmentinbroadbandinfrastructuredeployment.

Winkler, J., L. Dueñas-Osorio, R. Stein, and D. Subramanian. 2010. "Performance assessment of topologically diverse power systems subjected to hurricane events." *Reliab. Eng. Syst. Saf.* 95 (4): 323–336. https://doi.org/10.1016/j.ress.2009.11.002.